

pubs.acs.org/JCTC Article

Hitting the Trifecta: How to Simultaneously Push the Limits of Schrödinger Solution with Respect to System Size, Convergence Accuracy, and Number of Computed States

János Sarka* and Bill Poirier*



Cite This: J. Chem. Theory Comput. 2021, 17, 7732-7744



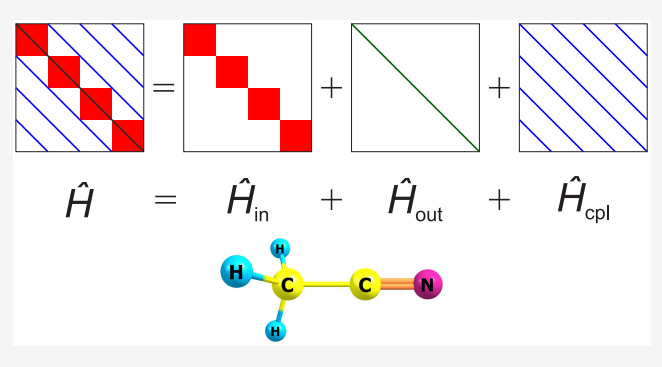
ACCESS

III Metrics & More

Article Recommendations

s Supporting Information

ABSTRACT: Methods for solving the Schrödinger equation without approximation are in high demand but are notoriously computationally expensive. In practical terms, there are just three primary factors that currently limit what can be achieved: 1) *system size/dimensionality*; 2) *energy level excitation*; and 3) *numerical convergence accuracy*. Broadly speaking, current methods can deliver on any two of these three goals, but achieving all three at once remains an enormous challenge. In this paper, we shall demonstrate how to "hit the trifecta" in the context of molecular vibrational spectroscopy calculations. In particular, we compute the lowest 1000 vibrational states for the six-atom acetonitrile molecule (CH₃CN), to a numerical convergence of accuracy 10^{-2} cm⁻¹ or



better. These calculations encompass all vibrational states throughout most of the dynamically relevant range (i.e., up to \sim 4250 cm⁻¹ above the ground state), computed in full quantum dimensionality (12 dimensions), to near spectroscopic accuracy. To our knowledge, no such vibrational spectroscopy calculation has ever previously been performed.

1. INTRODUCTION

Methods for solving the Schrödinger equation have seen an explosive growth in recent years, as the importance of incorporating quantum effects in numerical simulations in order to obtain experimentally accurate data becomes increasingly recognized. In the last two decades, the accurate solution of the nuclear-motion or (ro)vibrational Schrödinger equation, in particular, has started to become feasible-if not routine-for polyatomic molecular systems. This development has made "exact quantum dynamical" (QD) calculations possible for small polyatomic systems, allowing theoretical calculations to start catching up with extremely accurate experimental measurements. Today, in the field of highresolution molecular spectroscopy, experiment and quantum theory provide equally important and often complementary contributions to our understanding and thus strengthen each other.1,2

Spectroscopy is, of course, a universal tool and, as such, serves as a workhorse across a wide range of scientific disciplines. Even just in the vibrational context, these include low temperature and ultracold physics, atmospheric science and combustion chemistry, astrophysics and remote sensing, chemical physics and quantum chemistry, geochemistry and astrobiology, and quantum control and quantum computing, among others. Developing codes to perform rovibrational molecular spectroscopy calculations is thus not only useful for the considerable number of researchers working in these computational fields but

also impacts a much broader range of experimental communities, for whom accurate (ro)vibrational spectroscopic data is of vital importance.

On the other hand, performing numerically exact QD simulations of (ro)vibrational spectroscopy for specific molecular systems is notoriously computationally expensive-a situation that, to date, has greatly limited the applications to which such simulations can be applied. In practical terms, there are three main directions along which there is a need to push the limits of present-day technology. These are 1) system size, i.e., the number of degrees of freedom or dimensions (vibrational modes) that can be treated explicitly quantum mechanically; 2) energy excitation, the total number of accurately computed (ro)vibrational quantum states or energy levels; and 3) numerical accuracy, measured in terms of convergence with respect to all possible computational parameters such as basis size (i.e., the equivalent of what could be called the "complete basis set full configuration interaction limit" in the electronic structure realm).

Received: August 16, 2021 Published: November 11, 2021





Limitation 1) is, of course, very well-known, with six or more atoms (i.e., 12 or more explicit quantum dimensions) certainly regarded as the "frontier", at present. Limitation 2) is equally important but nowhere near as often concerned with-at least not within the realm of theoretical/numerical treatments. Experimentalists, however, know full well that six-or-more atom molecules can present anywhere from 10^3-10^7 , or even more, spectroscopically active (ro)vibrational bands. Even H₂⁺, the "smallest polyatomic molecule", presents a total of 390,855 bound rovibrational states.³ Benzene exhibits 1 million or so vibrational states lying below even just the first overtone of its highest fundamental!⁴⁻⁶ Therefore, a theoretical calculation that is restricted to tens or even a couple of hundred total computed states-or that focuses on just the fundamental frequencies-may, in practical terms, be of limited value. As for Limitation 3), of course, the definition of "spectroscopic accuracy" depends very much on the precise experimental apparatus, especially whether one is conducting infrared or microwave (pure rotation) experiments. A conservative rule-ofthumb estimate might be $10^{-\frac{1}{3}}$ cm⁻¹ or better—although for our purposes, we will regard a calculation that is numerically converged (with respect to all possible parameters) to better than 10^{-2} cm⁻¹ as achieving "high-resolution spectroscopic accuracy".

Broadly speaking, the current state-of-the-art numerical methodologies can deliver on pushing the limits of any two of the above three limitations, but achieving all three goals at once remains an enormous challenge. As a representative but incomplete summary, codes employing tensor methods as developed, e.g., by Carrington and co-workers⁷ and Martinez and co-workers, ^{8,9} can readily provide 1) and 3) together but not 2). In contrast, the *SwitchBLADE*^{4,10-13} code, developed in our group, can provide 1) and 2) together but not 3). Then, there are the "black-box" rovibrational molecular spectroscopy codes, such as $ScallT^{14-18}$ (also developed in our group), DOPI, ^{19–21} DEWE, 22-25 and GENIUSH 26,27 (developed in the group of Császár, the latter further developed by Mátyus and coworkers²⁸), *DVR3D*²⁹ (developed by Tennyson and coworkers), and *Trove*^{30,31} (developed by Yurchenko and coworkers). Due in some cases to design and in others to the canned direct-product basis sets (DPBs) and coordinate systems used by default, the black-box codes are typically limited in terms of 1), though they can provide 2) and 3) quite readily.

Of course, the above is a broad or typical characterization only—a panoramic snapshot of where things currently stand, for the most part. It must be recognized that development of all of the above methods is ongoing. Indeed, in this paper, we shall describe a combination strategy, wherein the "best of two worlds"-i.e., from the SwitchBLADE and ScalIT codes described above-is successfully merged together in order to achieve all three desired goals at the same time. We then apply the resultant combined code, which we call "SwitchIT", to a wellstudied benchmark system-the acetonitrile (CH₃CN) molecule.

In a nutshell, SwitchIT works as follows. Instead of using canned DPBs for all of the various system dimensions (as would be the default for ScalIT), the so-called "outer" group of dimensions is represented using a highly efficient, non-DPB of the SwitchBLADE form. The result is an exponentially smaller outer basis—yet one that still retains the sparse, block-structured matrix form necessary for *ScalIT* to function effectively. In this manner, SwitchIT defeats the traditional exponential scaling of computational cost (implied by the use of DPBs), while keeping the high accuracy and convenience that DPBs provide and also allowing for effective massive parallelization across near-exascale supercomputing clusters.

In this manner, we are able, in the present work, to "hit the trifecta" in our CH₃CN calculations. Specifically, we computed the lowest-lying 1000 vibrational energy levels of CH₃CN to spectroscopic numerical convergence accuracy, as defined above. Such calculations encompass all vibrational levels up to \sim 4250 cm⁻¹ above the ground state, which are computed here in full quantum dimensionality (12 dimensions). Such calculations are well beyond what has previously been achieved for this system. 12,32,33 Indeed, to our knowledge, no such vibrational spectroscopy calculation has ever previously been performed—at least not for a system with reasonably strong inherent coupling. On the other hand, given the generality and effectiveness of the method, we anticipate there will be many more such calculations to follow.

As our most immediate next step, we plan to extend the present CH₃CN investigation up to ten thousand vibrational states, all computed to near-spectroscopic accuracy. This will require a further modification to the SwitchIT code that incorporates a quadrature approximation for the "inner" dimensions-resulting in a sparser matrix form and, therefore, much larger possible matrix sizes. In the future, other molecular systems of spectroscopic interest will also be considered. More broadly, we hope to make our generic code available to the various scientific communities described above—thus extending spectroscopically relevant exact QD calculations to both larger and more general molecular systems than have heretofore been the case.

2. THEORY

The numerical challenges associated with computing more and more exact rovibrational eigenstates of molecules of increasing size, to increased levels of numerical convergence accuracy, increase very dramatically. To address these challenges, one can utilize massively parallel computers, such as high performance computing clusters (HPCCs), up to tens or even hundreds of thousands of cores. However, to effectively apply them, one needs to develop scalable algorithms—which presents its own set of challenges in the exact quantum dynamics context. Over the past two decades, two different massively parallel codes have been developed in our group to overcome those challenges.

In this section, we discuss the two established codes that are used in this study-i.e., SwitchBLADE and ScalIT-as well as how these can be most profitably combined together to form the new code, "SwitchIT". In this initial study, we consider only anharmonic force field (AFF) potential energy surfaces (PESs) and also certain refinements that are tailored for the CH₃CN molecules. However, the basic procedure may be applied more generally, to arbitrary PESs.

2.1. SwitchBLADE. SwitchBLADE, 4,10-13 Switchable Basis set Linear Algebra modules for Dimensionally independent Eigensolves, is a black-box code designed to implement highly efficient non-DPB representations. Whereas the individual basis functions are separable across all dimensions, the global truncation of the basis set itself is highly correlated-not only across all d configuration space dimensions but also, where applicable, across all 2d phase space dimensions. This highly correlated truncation of the basis can be finely tuned for specific applications, thus resulting in an exponential reduction in the required basis size, n. This, in turn, allows comparatively large systems (i.e., d values) to be tackled explicitly. As a result,

remarkably high (k/n) ratios may be obtained, where k is the number of states computed to a given accuracy threshold. ^{10,34}

An important feature of the *SwitchBLADE* approach is that *direct* methods are employed to solve the matrix eigenproblem. On the one hand, this offers a great advantage, in that LINPACK-like $ScaLAPACK^{35-37}$ parallel dense matrix linear algebra routines may be employed—of the precise sort that are routinely used to establish parallel scalability benchmarks across the largest supercomputers currently in existence. This all but ensures the effective parallel scalability of SwitchBLADE on any cluster, even using a combination of intranode (shared memory) and internode (distributed memory) parallelization (previously, up to 7200 cores have been used for a single job). There is also the advantage that all n eigenstates (or k converged eigenstates) are computed at once.

On the other hand, direct methods treat all matrices as dense (even if in reality this is not the case), requiring order n^2 storage. This means that the basis sizes n are limited by the largest matrices that can be directly diagonalized on currently available clusters—which is about $n \approx 10^6$. This is rather small, in comparison to the basis sizes that can be achieved using more specialized methods that exploit special matrix structure such as sparsity. Consequently, the numerical accuracy of the majority of the k converged levels is relatively low—i.e., only a few cm⁻¹ or tens of cm⁻¹, for the largest d values considered to date (up to d = 30).

The current *SwitchBLADE* code is limited to AFF (or related) PESs, although this is by no means an inherent limitation. In particular, the AFF restriction enables analytic determination of the PES matrix elements. Consequently, *SwitchBLADE* introduces no quadrature or other errors beyond basis set truncation, meaning that numerical convergence is fully variational from above. As for the basis functions themselves, *SwitchBLADE* was originally designed for phase-space-localized basis sets such as "weylets" and (momentum)-symmetrized Gaussians (SGs). 44–47 However, it has also been adapted for use with correlated truncated harmonic oscillator (HO) basis sets, as are used in this work. The HO basis is preferred here, because the lower lying states are much more accurately numerically converged [although (k/n) ratios are also much smaller]. 4,10–13

By now, *SwitchBLADE* has been successfully applied to uncoupled and coupled harmonic oscillator model problems and to various AFF PES molecules such as P₂O and CH₂NH, CH₃CN, benzene, and the OCHCO molecular ion. Also, a modified version of the algorithm used to apply phase space truncation to the SG basis of *SwitchBLADE* has been transformed into a new code, *CRYSTAL*, see used to detect and find "holes"—as well as legitimate transition states—in large-dimensional PESs.

2.2. ScalIT. *ScalIT*, ^{14–18} or "*Scalable Iteration*", is a black-box molecular rovibrational spectroscopy code, designed to provide highly accurate solutions to the time-independent, nuclear-motion Schrödinger equation—including those lying in the highly energetically excited region of the spectrum. Like *SwitchBLADE*—and as the first part of its name implies—*ScalIT*, too, was designed to scale effectively across massively parallel supercomputing clusters (to date, a few thousand cores have been used for a single job). The "*ITeration*" part of the name refers to *ScalIT*'s use of efficient sparse iterative matrix diagonalization methods, as opposed to the direct matrix methods used by *SwitchBLADE*. As a consequence, *ScalIT* can accommodate very large sparse matrices (up to $n \approx 10^9$ if not larger), provided they adhere to a certain sparse block structure

that arises naturally in the context of certain DPB representations such as discrete variable representations (DVRs; see section 2.4).⁵⁰

On the other hand, since the DPB restriction is always imposed, this could limit the system dimensionalities, d, that might be considered—especially when ScallT is run in "black box" mode, using standard coordinate systems and canned basis sets. There are, for instance, high-level ScallT modules designed specifically to compute the (ro)vibrational states of triatomic and tetraatomic molecules, using Jacobi coordinates, and standard associated Legendre polynomial or Wigner rotation function basis sets for the bend and rotation angles. In this context, ScallT calculations have been performed to date only up to d=8–e.g., in a calculation of the rovibrational states of the Ne $_4$ rare gas tetramer. Other such black-box ScallT calculations include (among others) the rovibrational states of HO_{2D}^{52-54} homonuclear (Ne $_3^{55}$ and Ar_3^{56}) and heteronuclear (Ne $_2Ar^{57}$ and Ar_2Ne^{58}) rare gas trimers, $SO_{2D}^{59}O_{3D}^{60,61}$ and H_3^{+62} as well as the vibrational states of acetylene (HCCH).

Even when running in "black box" mode, *ScalIT* automatically employs a few numerical optimization strategies, such as use of the phase-space optimized DVR (PSO–DVR) basis representation for all radial coordinates, ^{50,52,64–67} which minimizes the radial basis sizes required. In addition, the preconditioned inexact spectral transform (PIST) method, ^{68–70} working in conjunction with optimal separable basis (OSB) preconditioning ^{71–74} as applied to the standard iterative quasiminimal residual (QMR) algorithm, ^{15,40} ensures the ability of *ScalIT* to accurately compute even extremely energetically high-lying quantum states (e.g., the "vinylidene" states of HCCH⁷⁵). A very brief description of the above combination of methods is presented in the Appendix; many further details may be found in the references listed above.

Despite past successes as described above, it was always a part of *ScalIT*'s design that even more impressive achievements would be possible by running the code in "expert" mode. In practice, this means replacing *ScalIT*'s canned Hamiltonian matrix construction routines with customized codes that make use of highly efficient, correlated basis sets, designed for specific applications. Note that, whereas *ScalIT* does indeed rely inherently on DPBs, it does so only across *groups* of dimensions—or "effective" dimensions—that may be chosen nearly arbitrarily by the expert user. If, then, the goal is to impose as little DPB restriction on the basis set as possible (so as to result in the smallest *n* and largest *d* values), then the number of groups or effective dimensions should be reduced to the minimal value of just *two*.

2.3. *SwitchIT*: **Overview.** The above two-tiered approach is what is adopted in the merged *SwitchIT* code of the present work, as described in more detail in this subsection.

Note that the current bottleneck of *SwitchBLADE* is the comparatively small basis sizes *n* that can be worked with, mainly due to the use of direct dense matrix eigensolvers, as discussed—whereas the primary advantage is the flip side of the same coin, i.e., a remarkably efficient basis that defeats exponential scaling in principle. *ScalIT*, on the other hand, suffers from the exponential scaling of *n* with *d* (as do all DPB methods) but overall can handle far larger *n* values, due to its sparse matrix eigensolve algorithms.

How, then, should the codes be most profitably merged together? One simple and effective strategy is to introduce *SwitchBLADE* into *ScalIT*, rather than the other way around. More specifically, we run the two-tier version of *ScalIT*

described above, as the main code. However, instead of using canned basis sets to represent the two reduced-dimensional subsystem Hamiltonians, a *SwitchBLADE* HO representation is used. This has the advantage of greatly *reducing* the overall basis size that is required (in comparison to pure *ScalIT*) while, at the same time, greatly *expanding* the overall basis size that can be worked with (in comparison to pure *SwitchBLADE*). In this manner, we achieve the "best of both worlds".

Note that ScalIT's OSB routines give rise to an adiabatic approximation across the two dimension groups (subsystems), which are therefore *not* treated identically. We therefore give the two groups different names, i.e., "inner" and "outer", with individual basis functions of the former parametrized by quantum numbers of the latter. For definiteness, and consistency with earlier treatments, we refer collectively to the inner subsystem dimensions as "x" and the outer subsystem dimensions as "y".

In order to ensure the sparse block diagonal structure required by *ScalIT*, it is most convenient (but not necessary) to work with a DPB representation for the inner subsystem. The proconceptual purposes, this could be, e.g., a PSO DVR basis (i.e., a standard of black-box *ScalIT*, as discussed)—although in reality, we will wind up using something else (see the next subsection). In contrast, the outer subsystem basis is completely unconstrained and so is taken to consist of the eigenstates of the outer subsystem Hamiltonian. The outer subsystem diagonalization problem, in turn, is represented (and solved) using *SwitchBLADE*.

Note that optimal sparsity is obtained by having $n_{\rm in} \approx n_{\rm o}$, where $n_{\rm in/o}$ represents the size of the inner/outer basis, and $n=n_{\rm in}n_{\rm o}$. Given that $n_{\rm o}$ is tremendously reduced due to the use of *SwitchBLADE*, but $n_{\rm in}$ is not, maintaining such a balance requires that *most* dimensions be lumped into the outer, rather than inner, category. Conversely, the PSO basis sets are ideal for capturing anharmonic behavior, and so, the inner subsystem should consist of the dynamically most important dimensions. These are general guidelines, although the implementation as discussed in the next subsection is based on a slightly different set of considerations.

The above discussion presumes an inner-outer decomposition of the form

$$\hat{H}(x, y) = \hat{H}_x(x) + \hat{H}_y(y) + \hat{\Delta}(x, y), \text{ where}$$
 (1)

$$\begin{split} \hat{H}_{x}(x) &= \hat{T}_{x}(x) + \hat{V}_{x}(x), \\ \hat{H}_{y}(y) &= \hat{T}_{y}(y) + \hat{V}_{y}(y), \text{ and} \\ \hat{\Delta}(x, y) &= \hat{V}(x, y) - \hat{V}_{x}(x) - \hat{V}_{y}(y). \end{split}$$
 (2)

Here, \hat{T} represents kinetic energy operators, and \hat{V} represents potential energy operators, respectively.

Now, when represented in matrix form using the basis sets as described above, $\hat{H}_x(x)$ becomes a block-diagonal matrix, and $\hat{H}_y(y)$ becomes a "diagonal-block" (actually fully diagonal in this case) matrix. The both of these contributions are highly sparse. Of course, the most interesting case is the inner-outer coupling contribution, $\hat{\Delta}(x,y)$, presumed to have a potential energy form. As such, the matrix representation in the above basis is diagonal with respect to x but not y. This is what is meant by the "diagonal-block" form, and it is precisely what is needed by *ScalIT*.

2.4. *SwitchIT*: Quadrature, Normal Modes, and Subsystems. Now, on to some more technical details—including those particular to the CH₃CN application, for which a quartic AFF PES is employed (section 3). We point out first of all that the implementation as described in the previous subsection—like all DVR methods—is characterized by *quadrature error*, above and beyond basis set truncation error. When spectroscopically accurate calculations are desired, very often the former error comes to dominate the latter—a situation that greatly slows down numerical convergence. So,76–79 Consequently, there is an impetus toward reducing quadrature error as much as possible, even at the expense of using less efficient basis sets.

In the case of CH₃CN (and a good many other systems)—remarkably—an effective basis may be chosen in which almost all quadrature error vanishes, even as the sparse block-structured form required by **ScalIT** is retained. As a consequence, numerical convergence becomes nearly perfectly variational. However, explaining how to achieve this serendipitous state of affairs first requires a slight detour into a brief discussion of the various representations involved.

The conceptually simplest representation is the *variational* basis representation (VBR), for which a) the orthogonal basis functions are delocalized and b) the individual matrix elements are computed exactly. Therefore, for any given operator, the corresponding VBR matrix has no quadrature error. Now, if we diagonalize the VBR matrix representation of the coordinate operator \hat{x} itself, the resultant eigenvalues constitute the DVR grid points. The eigenvectors define a unitary transformation to a new set of basis functions—the DVR functions—that are localized and Dirac-delta-like.

Next, we introduce some evidently new notion. For any given operator, let the *finite variable representation* (FVR) denote the *exact* matrix representation in the DVR basis. Note that the FVR is unitarily equivalent to the VBR and thus also has no quadrature error. However, the FVR is not typically used in practice. Instead, a simplifying approximation is generally employed, involving the part of the operator that can be expressed as a function of coordinates (e.g., the potential energy contribution, in the case of Hamiltonian operators). Specifically, the approximation replaces the exact FVR for this function with a diagonal matrix consisting of the values of the function evaluated at the DVR grid points. The result—which is highly convenient but most definitely has quadrature error—is the *discrete variable representation* or DVR.

Now, in our approach, instead of using a PSO DVR to represent the inner subsystem, an exact FVR is used, based on a corresponding classical orthogonal polynomial (COP) DVR^{79-81} (Gauss-Hermite in our case). Of course, for a single power of x, the above discussion implies that the corresponding FVR and DVR matrices are identical. Put another way, the DVR has no quadrature error in this case—or conversely, the exact FVR is *diagonal*.

For a COP DVR, moreover, the quadrature error for x^2 is very well characterized and known to be "small" in some sense. Specifically, adding just one more quadrature point would eradicate the COP DVR quadrature error for x^2 completely. Now, keeping in mind that "x" actually denotes a collection of dimensions, $x = (x_1, x_2, ...)$, across which the FVR is actually a DPB, it becomes clear that any bilinear form such as x_1x_2 also admits an exact, diagonal representation in a DVR/FVR.

Next, we consider the C_{3v} symmetry of the CH₃CN molecule and the impact this has on the vibrational normal modes and the

quartic AFF PES. In general, we expect there to be a combination of singly degenerate modes (which are invariant under C_3 rotations) and doubly degenerate modes (which are not). In the case of CH₃CN, there are four modes of each degeneracy, giving rise to a total of 12 modes in all. We shall take the (4D) inner subsystem (x) to consist of the even-symmetric components of the four doubly degenerate modes, whereas the (8D) outer subsystem (y) will consist of the remaining four doubly degenerate components plus the four singly degenerate modes. Note that the outer subsystem dimensionality is much larger than that of the inner subsystem, as desired.

There are also important ramifications of this choice for quadrature, as we shall see. To understand this, we must first provide a precise definition of the effective inner and outer Hamiltonians in eq 2. This should be done in such a manner as to minimize quadrature. As we shall see, $\hat{H}_x(x)$ and $\hat{H}_y(y)$ shall be represented exactly, meaning that the only source of quadrature error comes from $\hat{\Delta}(x, y)$ —which should therefore be made as small as possible. As it happens, this is precisely the task of the PSO DVR methodology, i.e., to provide "optimal" inner and outer PESs from the standpoint of minimizing $\hat{\Delta}(x, y)$.

For an arbitrary PES, the optimal or PSO inner subsystem (x) PES is obtained by relaxing with respect to all outer dimensions (y) and vice versa. For any AFF PES, the inner and outer PSO PESs are not themselves AFFs, due to inner-outer correlation. However, the optimal PESs of AFF form can be shown to be simply $\hat{V}_x(x) = \hat{V}(x,0)$ and $\hat{V}_y(y) = \hat{V}(0,y)$. These are thus used to define $\hat{H}_x(x)$ and $\hat{H}_y(y)$.

2.5. SwitchIT: Matrix Representations. We now return to the issue of matrix representations for the two subsystems and their coupling, each of which must be treated separately. For the inner subsystem, the matrix representation of $\hat{H}_x(x)$ is exact (i.e., no quadrature error), since an exact Gauss-Hermite FVR is used. This is implemented in two steps. First, the $\hat{H}_x(x)$ Hamiltonian is represented in a DPB HO VBR of size $n_{\rm in} = n_1 n_2 n_3 n_4$, where n_1 is the number of basis functions used for dimension x_1 , etc. Then, the VBR matrix is transformed to the FVR, one dimension at a time, using the eigenvectors of the respective inner coordinate operators, $(\hat{x}_1, \hat{x}_2, \hat{x}_3, \hat{x}_4)$, as computed in the same HO VBR basis. We denote the resulting $n_{\rm in} \times n_{\rm in}$ matrix as $H_{\rm ii'}^{\rm ii'}$, where i labels a particular 4D inner Gauss-Hermite quadrature point, $(x_1^i, x_2^i, x_3^i, x_4^i)$.

The outer subproblem, $\hat{H}_y(y)$, is solved directly in *SwitchBLADE*, using a correlated truncated harmonic oscillator (HO) basis set (with a total basis size of $n_{\rm out}$). Note that since the outer PES is also of quartic AFF form, this representation is also *exact*, in the sense that it contributes no quadrature error. The eigenfunctions of the $\hat{H}_y(y)$ obtained from the direct matrix diagonalization—i.e., the $\phi_j(y)$ —serve as the outer basis for the final calculation and must therefore be stored. To this end, the standard *PDSYEV Scalapack* eigensolver of *SwitchBlade* has been changed to *PDSYEVR*. Of course, not all $n_{\rm out}$ eigenvectors are required, and only the lowest-lying $n_{\rm o} < n_{\rm out}$ eigenvectors are retained. That said, the ratio $(n_{\rm out}/n_{\rm o})$ is much smaller than might be expected for an 8D calculation, due to the inherent efficiency of the *SwitchBlade* calculation.

Finally, there is the inner-outer coupling contribution, $\hat{\Delta}(x, y)$. Here, the matrix representation *must* be diagonal in y-and, therefore, diagonal-block as a whole—in order to satisfying the sparse block structure required by *ScalIT*. Accordingly, we represent this contribution using a Gauss-Hermite DVR, rather than FVR, for the inner dimensions. There is, as a result, some

quadrature error that gets introduced; however, it is quite small, as may be seen as follows.

First, from the definition of $\hat{V}_x(x)$ and $\hat{V}_y(y)$, it is clear that every monomial term in $\hat{\Delta}(x,y)$ has at least one power of x and one power of y. Furthermore, since $\hat{\Delta}(x,y)$ is a quartic AFF, each term must be no less than first-order and no higher than third-order, in x or in y. Finally, by definition, the x coordinates are even-symmetric, implying that only second-order x factors contribute to any given $\hat{\Delta}(x,y)$ term. The coupling potential must therefore take the form

$$\hat{\Delta}(x, y) = \sum_{\alpha=1}^{\alpha_{\text{max}}} c_{\alpha}^{(3)} x^{2} y + \sum_{\beta=1}^{\beta_{\text{max}}} c_{\beta}^{(4)} x^{2} y^{2}$$
(3)

where $c_{\alpha}^{(3)}$ and $c_{\beta}^{(4)}$ are cubic and quartic force constants, respectively. Note that in eq 3, the expression x^2 refers to any possible product of inner dimensions, etc. For all second-order cross terms in x–e.g., the bilinear x_1x_2 –the quadrature is exact, as discussed previously. Only for the four x_1^2 -type terms is there any quadrature error at all, and even then it is small, because a COP DVR is employed.

Using the direct product of the inner FVR/DVR, and the outer basis, ϕ_i , the total Hamiltonian takes the matrix form

$$\mathbf{H}_{ii'jj'} = \mathbf{H}_{ii'}^{x} \delta_{jj'} + E_{j}^{y} \delta_{jj'} \delta_{ii'} + \mathbf{\Delta}_{jj'}(x_{i}) \delta_{ii'}$$

$$\tag{4}$$

where

$$\Delta_{jj'}(x_i) = \int \phi_{j'}(y) * \Delta(x_i, y) \phi_{j}(y) dy$$
(5)

The $\Delta_{jj'}(x_i)$ matrix representing the inner-outer coupling contribution, $\hat{\Delta}(x,y)$, can be obtained analytically, by evaluating the integral of eq 5 for each x_i inner grid point separately. The integrations are performed not using the $\phi_j(y)$ themselves but using the underlying HO basis functions in terms of which they are represented—for which analytic formulas are known. This requires a rectangular HO-to- ϕ transformation, involving the lowest-lying n_0 of n_{out} outer eigenfunctions, as discussed.

3. POTENTIAL ENERGY SURFACE (PES)

Previous vibrational state computations carried out for the CH₃CN system 12,32,33 utilized some version of the hybrid coupled cluster/DFT quartic AFF PES of Pouchan et al. 32 The harmonic part of this PES was computed using CCSD(T)/cc-pVTZ, while the cubic and quartic force constant coefficients were computed at the B3YLP/cc-pVTZ level. Although currently this is the best available potential for CH₃CN of which we are aware, its accuracy is limited—partially due to the fact that only force constant coefficient values larger than 6 cm $^{-1}$ were reported. Therefore, quantitative agreement (to spectroscopic accuracy) between our calculated energy levels and their experimental counterparts certainly cannot be expected. 82,83

A more serious concern is that some of the crucial implementational details needed to actually generate the Pouchan PES are absent from ref 32. In particular, coefficients are reported for only one set of components for the doubly degenerate modes—resulting in an effectively 8D rather than 12D PES. Thus, the PES must somehow be expanded for full 12D computations, which necessarily leads to ambiguity. Indeed, this has been done differently in two different previous vibrational state studies, ^{12,33} albeit consistent in both cases with the requisite Henry and Amat relations. ^{84–86}

Additionally, although the coefficients of the CH₃CN PES have been reported adopting an *unconstrained* summation

convention (USC) [i.e., labeling the third- and fourth-order coefficients as ϕ 's rather than the k's of the constrained summation convention (CSC)], the resultant PES exhibits a "hole" lying well below the zero-point vibrational energy (ZPVE). Such a PES is clearly unsuitable for a calculation of 1000 or more vibrational states! Accordingly, we have chosen to interpret the reported USC ϕ values as CSC k values. This has the effect of increasing the hole energy from ~7700 to 15 857 cm⁻¹, according to a recent calculation performed using our PES "hole finder" code, CRYSTAL. The motivation for this reinterpretation of the coefficients was the notion that CSC kvalues may have actually been what was originally intended—as is certainly the case, e.g., for the methylenimine (CH2NH) PES constructed by the same authors. 87 Although this turned out not to be the case for CH₃CN, it does not really matter; at the end of the day, the above procedure provides us with a viable benchmark 12D PES for the purpose at hand.

That said, PES ambiguity does make direct comparison with earlier vibrational state computations a bit tricky. In particular, Avila and Carrington computed³³ the lowest-lying 200 or so vibrational states, using the USC Pouchan PES and their own 8D-to-12D expansion scheme. Halverson and Poirier computed¹² 100 000 vibrational states using *SwitchBLADE*, albeit to much lower accuracy for the high-lying states. They also used the CSC Pouchan PES, with a different 8D-to-12D expansion scheme that is properly invariant with respect to permutations of the mode labels (unlike the approach used in ref 33).

Most of the SwitchIT results presented in this paper were computed using the CSC Pouchan PES with the permutationinvariant expansion scheme. In addition, we have taken advantage of developments in massively parallel supercomputers over the past few years, in order to redo the earlier SwitchBLADE computations of ref 12 (and also fix a small error)-specifically, using an HO basis with what is called the "square root" truncation (SQRT) scheme (section 4.1) in order to obtain an up-to-date comparison here. Finally, we have also performed one SwitchIT computation of the USC Pouchan PES, using the most converged basis set from the CSC computations. The latter enables a partially meaningful comparison with the earlier study of ref 33, although the two PESs used are still not identical, due to different 8D-to-12D expansion schemes. Note that complete specifications of both PESs used in this work are provided in the Supporting Information, which should go some way toward avoiding further such ambiguities in the future.

4. RESULTS AND DISCUSSION

4.1. Numerical Convergence. 4.1.1. 8D Outer Subsystem Convergence. We begin with a discussion of the numerical convergence of the 8D outer subsystem problem. Since this subsystem consists of just the odd-symmetric components of the four doubly degenerate modes, plus the four singly degenerate modes, the resultant $\hat{V}_y(y) = \hat{V}(0,y)$ 8D outer PES is simply the original unexpanded 8D PES as reported in ref 32 (albeit reinterpreted under a CSC). As discussed, the 8D outer subsystem problem is solved directly via **SwitchBLADE**, using a quadrature-free HO VBR representation.

The specific correlated truncation scheme used is the SQRT method, ¹² which appears to be the most suitable for our purpose of reaching high accuracy over the entire dynamically relevant energy range. In the SQRT scheme, the truncation weights, *w*, for individual normal modes are roughly proportional to the *square roots* of the normal-mode frequencies. A given 8D HO

basis function is then retained for the matrix representation of $\hat{H}_{v}(y)$ if and only if

$$w_1 j_1 + w_2 j_2 + \dots + w_7 j_7 + w_8 j_8 \le n_{\text{cut}}$$
 (6)

where j_1 labels the particular HO basis function used for dimension $y_1 = q_1$, etc., and the cutoff value n_{cut} is the sole numerical convergence parameter. Ordering the dimensions such that the singly degenerate modes come first, we have $y = (y_1, ..., y_8) = (q_1, q_2, q_3, q_4, q_{5y}, q_{6y}, q_{7y}, q_{8y})$ (see also the Supporting Information). The corresponding SQRT weights as applied here are $w = (w_1, ..., w_8) = (3, 3, 2, 2, 3, 2, 2, 1)$, respectively.

As discussed, the target 1000 12D vibrational states extend up to ~4250 cm⁻¹. For the 8D outer Hamiltonian, $\hat{H}_y(y)$, there are only 181 quantum states within this same energy range. To obtain a suitable outer basis, $\phi_j(y)$, we increased $n_{\rm cut}$ until those 181 states were all converged to around 0.01 cm⁻¹ or better. This required $n_{\rm cut}=26$, leading to a primitive 8D outer basis size of $n_{\rm out}=133$ 051. Anticipating that a few thousand $\hat{H}_y(y)$ eigenstates would be needed for the final 12D computation, we saved the lowest-lying 10 000, which is thus the maximum possible value for n_0 .

4.1.2. 4D Inner Subsystem Convergence. To represent the 4D inner subsystem (consisting of the even-symmetric components of the four doubly degenerate modes), we used a DPB Gauss-Hermite FVR. The target 12D energy range includes only 54 4D quantum states. Although obtaining the eigenvalues of the inner subsystem is not actually necessary for the full 12D computation *per se*, it nevertheless provides important insight about the convergence accuracy of the inner basis set, and so we performed such a calculation. Again, the goal was to compute all 54 of these lowest-lying 4D states to 0.01 cm⁻¹ or better.

The numerical convergence of the 4D inner subsystem problem was evaluated in two steps. First, a set of computations was performed for which each of the four individual basis sizes, (n_1, n_2, n_3, n_4) [or maximum excitations, (i_1, i_2, i_3, i_4)] was determined using eq 6. This enables convergence to be determined through a single parameter n_{cut} for which the value $n_{\text{cut}} = 25$ was found to be the smallest to achieve the desired convergence. Note that unlike the outer subsystem problem, the inner subsystem basis is not actually truncated via the SQRT scheme, as it is a "rectangular" or DPB basis. Instead, the SQRT weights are used to determine the individual DPB basis sizes, $(n_1, n_2, n_3, n_4) = (9, 13, 13, 26)$, corresponding respectively to the inner subsystem dimensions, $x = (x_1, x_2, x_3, x_4) = (q_{5x}, q_{6x}, q_{7x}, q_{8x})$. The total inner basis size is thus equal to the quadruple product, $n_{\text{in}} = n_1 n_2 n_3 n_4 = 39$ 546.

In the second numerical convergence step, the four n values listed above were varied individually, so as to reduce the total inner basis size $n_{\rm in}$, while still retaining the desired accuracy. In this manner, we were able to reduce the inner basis considerably, down to $(n_1, n_2, n_3, n_4) = (6, 6, 9, 22)$, and $n_{\rm in} = 7128$.

4.1.3. Inner-Outer Coupling and Full 12D Hamiltonian Matrix Diagonalization. The inner-outer coupling matrix, $\Delta_{jj'}(x_i)$, was obtained as described in section 2.5. This required combining the 4D Gauss-Hermite FVR code with the "Hamiltonian matrix builder" portion of the SwitchBLADE code. Creating the coupling matrix could be a few thousand times more expensive than creating the 8D—or even the 12D—Hamiltonian matrix of SwitchBLADE proper. Therefore, the Hamiltonian matrix builder code was tweaked to utilize sparsity so as to run much more efficiently. Even so, creating and

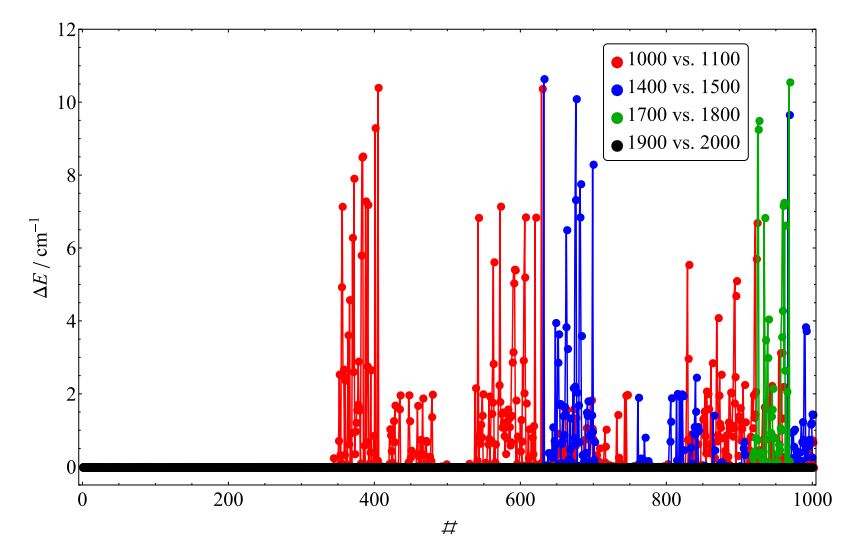


Figure 1. Numerical convergence of the lowest-lying 1000 vibrational energy levels of CH₃CN as computed using *SwitchIT* with the CSC Pouchan PES, with respect to the outer basis size, $n_{\rm o}$. $\Delta E = E_{\rm smaller} - E_{\rm larger}$.

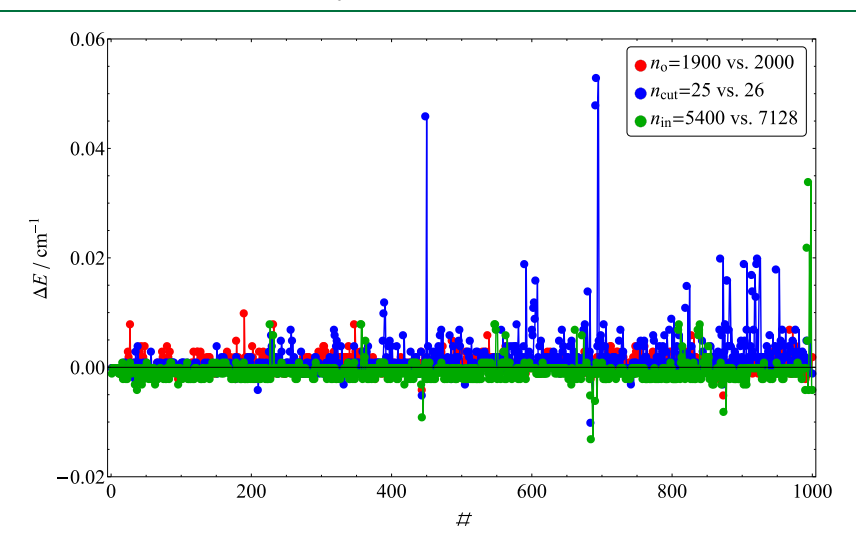


Figure 2. Numerical convergence of the lowest-lying 1000 vibrational energy levels of CH₃CN as computed using *SwitchIT* with the CSC Pouchan PES, with respect to the three convergence parameters: inner basis size $(n_{\rm in})$; primitive outer basis size used in 8D outer computation $(n_{\rm cut} = 25 \text{ and } 26 \text{ correspond to } n_{\rm out} = 105 \text{ 299 and } 133 \text{ 051, respectively})$; and final outer basis size used in full 12D computation $(n_{\rm o})$.

transforming $\Delta_{jj'}(x_i)$ still remains very demanding computationally; executing this step is comparable to the effort needed to diagonalize the full 12D Hamiltonian matrix.

As discussed, the diagonalization of the full 12D Hamiltonian matrix was carried out using *ScalIT*. Having only two-dimensional layers (i.e., inner and outer) reduces the overall sparsity and therefore the overall matrix sizes that can be implemented on the computing facilities at our disposal. Moreover, the comparatively large inner basis size, $n_{\rm in}$, results in slow OSB preconditioner construction—which sometimes made it difficult to complete the largest computations within our 48-h queue limitation. Nevertheless, for our final 12D eigenvalue computation, we were able to obtain all 1000 vibrational states from a single job, using a single PIST spectral window.

4.1.4. Full 12D Convergence. For the full 12D computation, a detailed convergence test was carried out involving all three numerical convergence parameters: inner basis size $(n_{\rm in})$; primitive outer basis size used in 8D outer computation $(n_{\rm out})$; and final outer basis size used in full 12D computation $(n_{\rm o})$. With regard to the two parameters also used in the subsystem

convergence tests, i.e., $n_{\rm in}$ and $n_{\rm out}$, the values needed to converge the full 12D computation turned out to be very similar to those needed for the subsystem problems as discussed above. With regard to $n_{\rm o}$, we find that $n_{\rm o} = 2000$ suffices to converge all 1000 12D vibrational states to less than 10^{-2} cm⁻¹.

Detailed convergence data with respect to n_0 is presented in Figure 1. Note that for a given basis size, there is a fairly sharp cutoff in the number of accurately converged states k, beyond which the convergence error suddenly increases from a tiny fraction of a cm⁻¹ up to 10 cm^{-1} or so. This pattern has been observed before and is what we refer to as the "efficiency cliff". ^{44–46} In any event, by $n_0 = 2000$, the cliff has moved beyond the first k = 1000 vibrational states, as desired.

In Figure 2, we present convergence data with respect to all three numerical convergence parameters. In particular, we report energy level differences between our best converged computation and the next best converged computation with respect to each of the three convergence parameters. The largest differences are in the 0.01–0.05 cm⁻¹ range. However, there are only a few of these large differences, and also they all correspond

Table 1. Selected Values for the Lowest-Lying 1000 Vibrational Energy Levels of CH₃CN, in cm⁻¹, as Computed Using SwitchIT with the CSC Pouchan PES, from Our Best Converged Calculation (Column 2)^a

no.	SwitchIT				SwitchBLADE	
	level	$\Delta(n_{\rm o}=1900)$	$\Delta(n_{\rm cut}=25)$	$\Delta(n_{\rm in}=5940)$	$\Delta(n_{\rm cut}=20)$	$\Delta(n_{\rm cut}=22$
1	9914.947	0.000	0.000	-0.001	0.00	0.00
2	363.470	0.000	0.000	0.000	0.00	0.00
3	363.471	0.000	0.000	0.000	0.00	0.00
4	728.460	0.000	0.000	0.000	0.00	0.00
5	728.460	0.000	0.000	0.000	0.00	0.00
5	729.929	0.000	0.000	0.000	0.00	0.00
7	907.005	0.000	0.000	0.000	0.00	0.00
3	1052.366	0.000	0.000	0.000	0.00	0.00
)	1052.366	0.000	0.000	0.000	0.00	0.00
10	1094.949	0.000	0.000	0.000	0.03	0.00
11	1094.950	0.000	0.000	-0.001	0.03	0.00
12	1097.855	-0.001	0.000	-0.001	0.03	0.00
13	1097.856	-0.001	0.000	-0.001	0.03	0.00
14	1269.787	-0.001	0.000	0.000	0.03	0.00
15	1269.813	0.000	0.000	0.000	0.01	-0.02
16	1399.899	0.000	0.000	0.001	-0.03	-0.03
17	1415.745	0.000	-0.001	-0.002	0.02	-0.01
18	1415.823	0.000	0.001	-0.001	0.03	0.00
19	1415.840	0.000	-0.001	-0.001	0.02	-0.02
20	1415.862	0.000	0.001	-0.001	0.03	0.00
21	1462.923	-0.001	-0.001	-0.002	0.03	0.00
22	1462.925	0.001	0.000	-0.001	0.03	0.00
23	1467.234	-0.001	-0.001	-0.002	0.03	0.00
24	1467.247	0.003	-0.001	0.000	0.02	-0.01
25	1468.681	0.002	0.000	0.000	0.02	-0.01
26	1486.895	0.001	0.000	-0.001	0.00	0.00
27	1486.923	0.008	0.000	0.001	-0.03	-0.03
28	1634.114	0.000	0.001	0.000	0.02	-0.01
29	1634.123	-0.001	-0.001	-0.001	0.01	-0.02
30	1635.581	0.000	0.000	0.000	0.02	-0.02
100	2460.983	0.000	0.000	-0.002	0.02	0.02
200	2893.310	0.000	0.002	-0.002	0.08	0.02
300	3237.703	0.002	0.000	0.000	0.05	0.00
400	3424.543	0.000	0.000	-0.002	0.10	0.07
500	3633.657	0.001	0.004	0.000	0.22	0.15
500	3767.138	0.000	0.001	0.000	0.08	0.05
700	3919.836	0.001	0.000	-0.001	0.42	0.05
800	4015.580	0.003	0.007	0.000	0.18	0.07
900	4104.314	0.000	0.001	-0.001	0.56	0.07
1000	4236.126	0.002	-0.001	-0.004	0.20	0.02

"The first entry denotes the ground state ZPVE, whereas subsequent entries are frequencies (energy differences) relative to the ground state. Columns 3–5 present numerical convergence data, in the form of differences relative to the penultimate calculations as presented in Figure 2. Columns 6 and 7 present differences relative to *SwitchBLADE* calculations, as presented in Figure 3.

to the very large change in $n_{\rm out}$ that occurs as $n_{\rm cut}$ is incremented from 25 to 26. Also, it should be borne in mind that these errors characterize the *penultimate* computation (in this case, $n_{\rm cut}$ = 25), not the final computation. Note that, due to the very small quadrature error, we are still very much in the regime where basis set truncation error dominates. This means that even small basis size changes lead to large reductions in truncation errors—as a result of which, we are fairly confident that our final values are indeed all converged to within 0.01 cm⁻¹. In any event, errors presented in Figure 2 with respect to the other two convergence parameters, $n_{\rm in}$ and $n_{\rm o}$, are already sufficiently small in almost every single case.

4.2. Full 12D Energy Levels and Comparison with Previous Results. 4.2.1. Full 12D Energy Levels. Selected

energy levels as computed using our most converged basis set $(n_{\rm in}=7128,\,n_{\rm cut}=26$ with $n_{\rm out}=133\,051,\,{\rm and}\,n_{\rm o}=2000)$ and their individual convergence data (given as energy level differences with the penultimate calculations of Figure 2) are listed in Table 1. Note that a comprehensive list of *all* 1000 computed energy levels is provided in the Supporting Information. From Table 1, we find most of the energy differences to be *much* less than $10^{-2}\,{\rm cm}^{-1}$ –closer to $10^{-3}\,{\rm cm}^{-1}$, in fact, even for the 1000th state.

4.2.2. Comparison with SwitchBLADE Calculations. As discussed, there is an interest in comparing the present SwitchIT data with the corresponding results obtained from a straight SwitchBLADE computation. At the time that ref 12 was written, we were only able to extend the HO SQRT SwitchBLADE

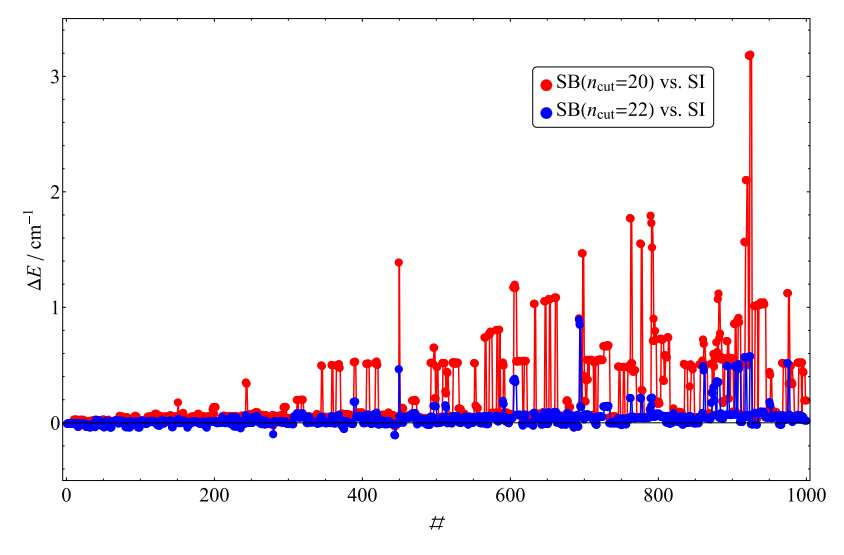


Figure 3. Energy level differences of the lowest-lying 1000 vibrational energy levels of CH₃CN as computed using HO SQRT *SwitchBLADE* (SB) and compared to the most converged *SwitchIT* computations (SI), for the CSC Pouchan PES. The two different SB n_{cut} values considered, i.e., $n_{\text{cut}} = 20$ and $n_{\text{cut}} = 22$, correspond to basis sizes $n = 582\ 150$ and $n = 1\ 211\ 394$, respectively.

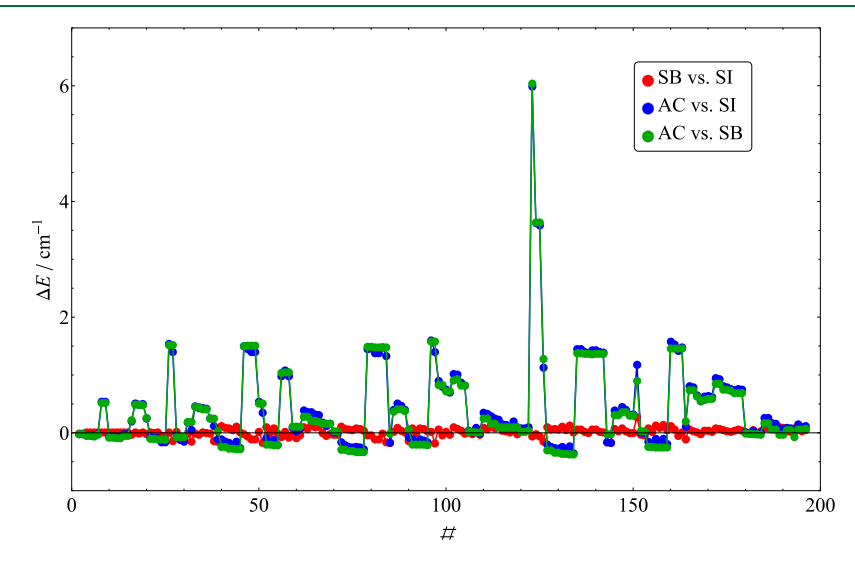


Figure 4. Energy level differences of the lowest-lying 200 vibrational energy levels of CH₃CN as computed using three different computations: Avila and Carrington, Jr. (AC); ³³ present *SwitchIT* (SI); and present *SwitchBLADE* (SB) with $n_{\text{cut}} = 22$. In all three cases, USC Pouchan PESs are used; however, the SI and SB USC PES are somewhat different from the AC USC PES.

computations out to $n_{\rm cut} = 20$. This corresponds to a total basis size of $n = 582\ 150$, divided into even and odd symmetry blocks of $n_e = 293\ 395$ and $n_o = 288\ 755$ basis functions, respectively. In the present study, we were able to extend these calculations out to $n_{\rm cut} = 22$, for which the corresponding basis sizes more than double (i.e., $n = 1\ 211\ 394$, $n_e = 609\ 471$, and $n_o = 601\ 923$). The latter calculation required around 20 h and 3500 cores per symmetry block, running on the Frontera cluster. Note that all 1000 of the computed lowest-lying HO SQRT *SwitchBLADE* energy levels are also provided in the Supporting Information.

It should be noted that the above $n_{\rm cut}$ values are substantially smaller than the $n_{\rm cut}=26$ value used in the most converged *SwitchIT* calculations! We therefore fully expect that for the *SwitchBLADE* calculations, the efficiency cliff will occur at k values far smaller than 1000—although the $n_{\rm cut}=22$ case should be substantially better than the $n_{\rm cut}=20$ case. Indeed, this is the reason why *SwitchBLADE* much more readily delivers on goals 1) and 2) from section 1 but not 3).

The above expectations are indeed found to hold true, as can be seen in Figure 3, as well as in the last two columns of Table 1. Here, we present computed energy level differences for the two HO SQRT *SwitchBLADE* computations, relative to the most converged *SwitchIT* computation of this study. To begin with, the largest differences are all positive (with *SwitchIT* energy levels being lower)—again indicating that basis set truncation error dominates. The largest errors are also on the order of several cm⁻¹, indicating the undesirable "top" of the efficiency cliff. For $n_{\text{cut}} = 20$, around 50 states have errors larger than 1 cm⁻¹, but also only around 50 states have errors less than 0.01 cm⁻¹. For $n_{\text{cut}} = 22$, the agreement is significantly better, with more than 250 states having errors less than 0.01 cm⁻¹.

Of course, these are not the *lowest* 250 states! In practical terms, one cannot predict which states they are, without doing a more accurately converged computation, as we have done here using *SwitchIT*. As a final comment on the *SwitchBLADE* study, we point out that *if* an HO SQRT *SwitchBLADE* computation with $n_{\text{cut}} = 26$ could be performed, it might be able to provide

similar accuracy as the *SwitchIT* computation presented here. Is such a computation feasible? We can actually compute the necessary basis sizes, i.e., n = 4618092, $n_e = 2318231$, and $n_o = 2299861$. Given the n^3 scaling of the direct matrix methods used by *SwitchBLADE*, this lies beyond our current computing capabilities—thus further justifying the *SwitchIT* approach.

4.2.3. Comparison with Avila and Carrington, Jr. In order to compare with the earlier study of Avila and Carrington, Jr., 33 we must work with the USC Pouchan PES for CH₃CN rather than the CSC version. Even then, the PES used here is *not* identical to that used in ref 33, as discussed in section 3. Rather than undertake a completely new convergence study for the USC case, we simply reused the most converged basis from the CSC Pouchan PES computation. As an additional check, to ensure that the results are not completely off the mark, we also performed an HO SQRT *SwitchBLADE* computation for the USC PES, using $n_{\text{cut}} = 22$. Note that Avila and Carrington, Jr. only computed the lowest-lying 200 energy levels, for which Figure 3 suggests the above *SwitchBLADE* computation ought to perform reasonably well. (Note that a USC version of Figure 3 may be found as Figure S1 of the Supporting Information.)

In Figure 4, we present energy differences for the lowest 200 energy levels of the USC Pouchan PES, as obtained from the three different computations, i.e., Avila and Carrington, Jr. (AC); present SwitchIT (SI); and present SwitchBLADE (SB). As is clear from Figure 4, SI and SB agree to within 0.1 cm⁻¹ or so for almost all levels, as expected, suggesting a corresponding level of numerical convergence for these calculations. The agreement of SI and SB with AC is also quite good, however, considering that the two PESs are, in fact, different. In particular, it is clearly visible from the figure that around half of the levels agree to better than 0.25 cm⁻¹-which is noteworthy, given that AC only claims to achieve a convergence of 0.2 cm⁻¹ or so and even then only for the lowest-lying 40 energy levels. There are several energy levels, however, with differences of around 1.5 cm⁻¹ and also three adjacent levels with differences in the 3.5-6.0 cm⁻¹ range. The regularity of these discrepancies suggests to us that they are most likely primarily due to excitations in one or two specific modes.

As a final note, one might also consider a comparison with the vibrational energy levels as computed in the original PES paper of Pouchan and co-workers.³² However, differences here are so great that one cannot even conclude which of the two Pouchan PES interpretations, USC or CSC, is the more likely. AC has also concluded that meaningful comparison with the energy level results of ref 32 is not possible.³³

5. CONCLUSIONS

Our goal for this project was to compute each and every one of the lowest-lying 1000 vibrational states of CH₃CN, in full quantum dimensionality (12D), to an overall numerical convergence accuracy of 10⁻² cm⁻¹ or better. This goal has been achieved, using the *SwitchIT* approach. Note that although only energy level results are presented here, it would also be straightforward to extract *eigenfunctions* using our existing code, if these were needed. In any event, this study represents the first time that *every* vibrational state within the most dynamically relevant range (~4250 cm⁻¹ in this case) of a six-or-more-atom molecule has been computed to spectroscopic accuracy, to our knowledge. Especially when combined with recent developments in highly accurate PES construction, ⁸⁸⁻⁹¹ we fully expect such capability to usher in a new era in rovibrational molecular spectroscopy—wherein comprehensive, experimentally relevant

spectroscopic line lists can be generated *ab initio* for much larger molecules than previously envisioned.

The three goals described above are highly desirable, as they represent the limits of modern-day computational molecular spectroscopy. As discussed in section 1, there are a number of codes and methods that can achieve any two out of threeincluding two prior codes developed by the authors, i.e., SwitchBLADE and ScalIT. Until now, however, none have been able to deliver the "trifecta". The success of SwitchIT in this regard is directly due to its ability to combine SwitchBLADE and ScalIT in such a way as to achieve the "best of both worlds". In particular, SwitchIT profits from the highly efficient correlated basis representations of the former, while still exploiting the sophisticated sparse matrix structure and eigensolver algorithms of the latter. Note that for comparison's sake, an up-to-date SwitchBLADE computation was also performed for the same CH₃CN system-which was found to have errors as high as 1 cm⁻¹ for some of the lowest-lying 1000 energy levels. *SwitchIT*, then, appears to go beyond what is possible using other codes.

In any event, the study conducted here represents only the beginning of what *SwitchIT* has to offer. For our next project, we plan to extend the range of near-spectroscopically accurately computed CH₃CN energy levels up to the first *ten thousand* states—which lie energetically up to around 6550 cm⁻¹ above the ground state. For this calculation, it is possible that the lowest-lying hole of the CSC Pouchan PES, located at 15 857 cm⁻¹⁴⁸ (i.e., 5942 cm⁻¹ above the ground state), might cause problems. This state of affairs might require yet another PES modification. On the other hand, the *SwitchIT* calculations performed here for the USC Pouchan PES suggest that the situation might also be workable as is. In any event, HO basis sets are far less amenable to damage caused by PES holes than are SG basis sets.

The upcoming 10 000-state CH₃CN study will also require some additional code development. At present, *SwitchIT* divides a given molecular system into two parts: the "inner" subsystem, consisting of the dynamically most important dimensions, represented in a Gauss-Hermite or other FVR/DVR, and the "outer" subsystem, represented using highly correlated *Switch-BLADE* basis sets (HO or SG). In this representation, the inner-outer coupling contribution to the Hamiltonian takes on the requisite "diagonal block" form, even as the inner and outer subsystem Hamiltonians are represented exactly.

Going forward, however, the larger basis sizes necessary to reach $k=10\,000$ states will necessitate a matrix with more sparsity—and, therefore, more dimensional layers. This will be achieved by subpartitioning the inner subsystem, at the expense of introducing additional quadrature error, through the innersubsystem coupling contributions. The increased quadrature error will necessitate larger $n_{\rm in}$ values—but then, much larger $n_{\rm in}$ and $n_{\rm o}$ values will now also become possible. Another, more minor difference from the computations performed here is that computing all 10 000 states will require multiple PIST spectral windows.

Of course, once the 10 000-state calculation of CH₃CN described above is completed, other molecular systems of spectroscopic interest will also be considered. Other *types* of calculations will also be considered—e.g., of the *rovibrational* states. Within the context of the existing *SwitchIT* codes, the addition of rotational degrees of freedom would be most easily accommodated using the Eckart-Watson formalism. ^{24,25} This would, however, entail a certain amount of new coding.

APPENDIX

Iterative eigensolvers such as Lanczos operate by building a "Krylov subspace" from successive multiplications of an arbitrary (typically random) starting vector by the Hamiltonian matrix, \mathbf{H} . These matrix—vector product operations are fast if \mathbf{H} is sparse, as is presumed. Moreover, only O(k) such multiplications are needed to compute the lowest k eigenvalues. This situation is highly favorable if $k \ll n$, but our goal is to go beyond Limitation 2).

To this end, we can apply Lanczos to the matrix $(EI - H)^{-1}$ rather than to H. The resultant calculation quickly converges the target eigenvalues closest to the energy E, which can be chosen anywhere in the spectrum. This is the basis of PIST. 68-70 Of course, the matrix $(EI - H)^{-1}$ itself is not known and not sparse. So, the action of the matrix on a vector, $\mathbf{w} = (E\mathbf{I} - \mathbf{H})^{-1}\mathbf{v}$, is simulated numerically via the linear solve problem, (EI - H)w =v, where w is the unknown vector. In practice, sparse iterative Krylov solvers are used, such as the generalized minimal residual method (GMRES)^{39,42} and QMR. ^{18,40} These methods optimize the expansion coefficients for a particular solution vector by employing a minimization or projection procedure at each Krylov iteration. For the present bound-state-calculation purpose, either GMRES or QMR is suitable, although QMR is better suited, in general, e.g., for resonance and scattering calculations. 69,70

Implemented as described above, the number of linear solve iterations becomes very large in practice, when E is high up in the spectrum. To greatly reduce this number, preconditioning is employed. Preconditioning consists of multiplying the linear-solve matrix $(E\mathbf{I} - \mathbf{H})$ by an *approximate* inverse (that can be inexpensively computed), in order to minimize the condition number of the product matrix. In particular, OSB preconditioning $^{71-74}$ uses an optimized adiabatic approximation that preserves the sparse block-structured form required by *ScalIT*.

ASSOCIATED CONTENT

Supporting Information

The Supporting Information is available free of charge at https://pubs.acs.org/doi/10.1021/acs.jctc.1c00824.

The lowest-lying 1000 vibrational energy levels of CH3CN computed in this work using the CSC PES with SwitchIT and SwitchBLADE (TXT)

The lowest-lying 1000 vibrational energy levels of CH3CN computed in this work using the USC PES with SwitchIT and SwitchBLADE (TXT)

Full 12D quartic AFF PES coefficients for CSC Pouchan PES of CH3CN (TXT)

Full 12D quartic AFF PES coefficients for USC Pouchan PES of CH3CN (TXT)

List of acronyms, full 12D quartic AFF PES coefficients for both CSC and USC Pouchan PESs for CH₃CN, as well as corresponding lowest-lying 1000 vibrational energy levels, as computed in this work using *SwitchIT* and *SwitchBLADE* (PDF)

AUTHOR INFORMATION

Corresponding Authors

János Sarka — Department of Chemistry and Biochemistry, Texas Tech University, Lubbock, Texas 79409, United States; orcid.org/0000-0003-4269-0727; Email: Janos.Sarka@ttu.edu Bill Poirier — Department of Chemistry and Biochemistry, Texas Tech University, Lubbock, Texas 79409, United States; orcid.org/0000-0001-8277-746X; Email: Bill.Poirier@ttu.edu

Complete contact information is available at: https://pubs.acs.org/10.1021/acs.jctc.1c00824

Notes

The authors declare no competing financial interest.

ACKNOWLEDGMENTS

J.S. would like to thank MolSSI for their support provided through the MolSSI Software "Seed" Fellowships (OAC-1547580). This work was supported by the National Science Foundation (CHE-1665370) and the Robert A. Welch Foundation (D-1523). The authors also gratefully acknowledge the Texas Tech University High Performance Computing Center for the use of the Quanah cluster and the Texas Advanced Computing Center for the use of the Lonestar5 and Frontera clusters.

REFERENCES

- (1) Pavanello, M.; Adamowicz, L.; Alijah, A.; Zobov, N. F.; Mizus, I. I.; Polyansky, O. L.; Tennyson, J.; Szidarovszky, T.; Császár, A. G.; Berg, M.; Petrignani, A.; Wolf, A. Precision Measurements and Computations of Transition Energies in Rotationally Cold Triatomic Hydrogen Ions up to the Midvisible Spectral Range. *Phys. Rev. Lett.* **2012**, *108*, 023002.
- (2) Pavanello, M.; Adamowicz, L.; Alijah, A.; Zobov, N. F.; Mizus, I. I.; Polyansky, O. L.; Tennyson, J.; Szidarovszky, T.; Császár, A. G. Calibration-quality adiabatic potential energy surfaces for H_3^+ and its isotopologues. *J. Chem. Phys.* **2012**, *136*, 184303.
- (3) Jaquet, R.; Carrington, T., Jr. Using a Nondirect Product Basis to Compute J > 0 Rovibrational States of H_3^+ . *J. Phys. Chem. A* **2013**, *117*, 9493–9500.
- (4) Halverson, T.; Poirier, B. One Million Quantum States of Benzene. J. Phys. Chem. A 2015, 119, 12417–12433.
- (5) Di Liberto, G.; Conte, R.; Ceotto, M. "Divide and conquer" semiclassical molecular dynamics: A practical method for spectroscopic calculations of high dimensional molecular systems. *J. Chem. Phys.* **2018**, *148*, 014307.
- (6) Wang, S. Intrinsic molecular vibration and rigorous vibrational assignment of benzene by first-principles molecular dynamics. *Sci. Rep.* **2020**, *10*, 17875.
- (7) Thomas, P. S.; Carrington, T. Using Nested Contractions and a Hierarchical Tensor Format To Compute Vibrational Spectra of Molecules with Seven Atoms. *J. Phys. Chem. A* **2015**, *119*, 13074–13091.
- (8) Parrish, R. M.; Hohenstein, E. G.; Schunck, N. F.; Sherrill, C. D.; Martínez, T. J. Exact Tensor Hypercontraction: A Universal Technique for the Resolution of Matrix Elements of Local Finite-Range N-Body Potentials in Many-Body Quantum Problems. *Phys. Rev. Lett.* **2013**, *111*, 132505.
- (9) Kokkila Schumacher, S. I. L.; Sara, I.; Hohenstein, E.; Parrish, R.; Wang, L. P.; Martínez, T. Tensor hypercontraction second-order Møller—Plesset perturbation theory: Grid optimization and reaction energies. *J. Chem. Theory Comput.* **2015**, *11*, 3042.
- (10) Halverson, T.; Poirier, B. Accurate Quantum Dynamics Calculations Using Symmetrized Gaussians on a Doubly Dense Von Neumann Lattice. *J. Chem. Phys.* **2012**, *137*, 224101.
- (11) Halverson, T.; Poirier, B. Calculation of exact vibrational spectra for P_2O and CH_2NH using a phase space wavelet basis. *J. Chem. Phys.* **2014**, *140*, 204112.
- (12) Halverson, T.; Poirier, B. Large scale exact quantum dynamics calculations: Ten thousand quantum states of acetonitrile. *Chem. Phys. Lett.* **2015**, *624*, 37–42.

- (13) Pandey, A.; Poirier, B. Using phase-space Gaussians to compute the vibrational states of OCHCO⁺. *J. Chem. Phys.* **2019**, *151*, 014114.
- (14) Chen, W.; Poirier, B. Parallel Implementation of Efficient Preconditioned Linear Solver for Grid-based Applications in Chemical Physics: I. Block-Jacobi diagonalization. *J. Comput. Phys.* **2006**, 219, 185–197.
- (15) Chen, W.; Poirier, B. Parallel Implementation of Efficient Preconditioned Linear Solver for Grid-based Applications in Chemical Physics: II. QMR linear solver. *J. Comput. Phys.* **2006**, *219*, 198–209.
- (16) Chen, W.; Poirier, B. Parallel Implementation of Efficient Preconditioned Linear Solver for Grid-based Applications in Chemical Physics: III. Improved parallel scalability for sparse matrix-vector products. J. Parallel Distrib. Comput. 2010, 70, 779–782.
- (17) Chen, W.; Poirier, B. Quantum Dynamics on Massively Parallel Computers: Efficient numerical implementation for preconditioned linear solvers and eigensolvers. *J. Theor. Comput. Chem.* **2010**, *9*, 825.
- (18) Petty, C.; Poirier, B. Using ScalIT for Performing Accurate Rovibrational Spectroscopy Calculations for Triatomic Molecules: A practical guide. *Appl. Math.* **2014**, *5*, 2756–2763.
- (19) Czakó, G.; Furtenbacher, T.; Császár, A. G.; Szalay, V. Variational vibrational calculations using high-order anharmonic force fields. *Mol. Phys.* **2004**, *102*, 2411–2423.
- (20) Furtenbacher, T.; Czakó, G.; Sutcliffe, B. T.; Császár, A. G.; Szalay, V. The methylene saga continues: Stretching fundamentals and zero-point energy of \tilde{X}^3B_1 CH₂. *J. Mol. Struct.* **2006**, 780–781, 283–294
- (21) Szidarovszky, T.; Császár, A. G.; Czakó, G. On the efficiency of treating singularities in triatomic variational vibrational computations. The vibrational states of H_3^+ up to dissociation. *Phys. Chem. Chem. Phys.* **2010**, *12*, 8373–8386.
- (22) Mátyus, E.; Czakó, G.; Sutcliffe, B. T.; Császár, A. G. Vibrational energy levels with arbitrary potentials using the Eckart-Watson Hamiltonians and the discrete variable representation. *J. Chem. Phys.* **2007**, *127*, 084102.
- (23) Mátyus, E.; Šimunek, J.; Császár, A. G. On the variational computation of a large number of vibrational energy levels and wave functions for medium-sized molecules. *J. Chem. Phys.* **2009**, *131*, 074106.
- (24) Mátyus, E.; Fábri, C.; Szidarovszky, T.; Czakó, G.; Allen, W. D.; Császár, A. G. Assigning quantum labels to variationally computed rotational-vibrational eigenstates of polyatomic molecules. *J. Chem. Phys.* **2010**, *133*, 034113.
- (25) Fábri, C.; Mátyus, E.; Furtenbacher, T.; Mihály, B.; Zoltáni, T.; Nemes, L.; Császár, A. G. Variational quantum mechanical and active database approaches to the rotational-vibrational spectroscopy of ketene. *J. Chem. Phys.* **2011**, *135*, 094307.
- (26) Mátyus, E.; Czakó, G.; Császár, A. G. Toward black-box-type fulland reduced-dimensional variational (ro)vibrational computations. *J. Chem. Phys.* **2009**, *130*, 134112.
- (27) Fábri, C.; Mátyus, E.; Császár, A. G. Rotating full- and reduceddimensional quantum chemical models of molecules. *J. Chem. Phys.* **2011**, *134*, 074105.
- (28) Avila, G.; Mátyus, E. Toward breaking the curse of dimensionality in (ro)vibrational computations of molecular systems with multiple large-amplitude motions. *J. Chem. Phys.* **2019**, *150*, 174107.
- (29) Tennyson, J.; Kostin, M. A.; Barletta, P.; Harris, G. J.; Polyansky, O. L.; Ramanlal, J.; Zobov, N. F. DVR3D: a program suite for the calculation of rotation—vibration spectra of triatomic molecules. *Comput. Phys. Commun.* **2004**, *163*, 85–116.
- (30) Yurchenko, S. N.; Thiel, W.; Jensen, P. Theoretical ROVibrational Energies (TROVE): A robust numerical approach to the calculation of rovibrational energies for polyatomic molecules. *J. Mol. Spectrosc.* **2007**, 245, 126.
- (31) Yurchenko, S. N.; Yachmenev, A.; Ovsyannikov, R. I. Toward black-box-type full- and reduced-dimensional variational (ro)-vibrational computations. *J. Chem. Theory Comput.* **2017**, *13*, 4368–4381.

- (32) Begue, D.; Carbonniere, P.; Pouchan, C. Calculations of vibrational energy levels by using a hybrid ab initio and DFT quartic force field: application to acetonitrile. *J. Phys. Chem. A* **2005**, *109*, 4611–4616.
- (33) Avila, G.; Carrington, T., Jr. Using nonproduct quadrature grids to solve the vibrational Schrödinger equation in 12D. *J. Chem. Phys.* **2011**, *134*, 054126.
- (34) Shimshovitz, A.; Tannor, D. J. Phase-Space Approach to Solving the Time-Independent Schrödinger Equation. *Phys. Rev. Lett.* **2012**, 109, 070402.
- (35) Choi, J.; Dongarra, J.; Pozo, R.; Walker, D. ScaLAPACK: a scalable linear algebra library for distributed memory concurrent computers. The Fourth Symposium on the Frontiers of Massively Parallel Computation. Los Alamitos, CA, USA, 1992; pp 120–127.
- (36) Blackford, L. S.; Choi, J.; Cleary, A.; D'Azevedo, E.; Demmel, J.; Dhillon, I.; Dongarra, J.; Hammarling, S.; Henry, G.; Petitet, A.; Stanley, K.; Walker, D.; Whaley, R. C. *ScaLAPACK Users' Guide*; Society for Industrial and Applied Mathematics: Philadelphia, PA, 1997; DOI: 10.1137/1.9780898719642.
- (37) of Tennessee, U.; Univ. of California, B.; of Colorado Denver, U.; Ltd., N. ScaLAPACK Scalable Linear Algebra PACKage. 2019. https://www.netlib.org/scalapack (accessed 2021-11-05).
- (38) Cullum, J. K.; Willoughby, R. A. Lanczos Algorithms for Large Symmetric Eigenvalue Computations; Birkhäuser: Boston, 1985.
- (39) Saad, Y.; Schultz, M. H. GMRES: a generalized minimal residual algorithm for solving nonsymmetric linear systems. *SIAM J. Sci. Statist. Comput.* **1986**, *7*, 856.
- (40) Freund, R. W.; Nachtigal, N. M. QMR: a quasi-minimal residual method for non-Hermitian linear systems. *Numer. Math.* **1991**, *60*, 315.
- (41) Golub, G. H.; Van Loan, C. F. *Matrix Computations*; The Johns Hopkins University Press: Baltimore, 1996.
- (42) Saad, Y. Iterative Methods for Sparse Linear Systems; Society for Industrial and Applied Mathematics: Philadelphia, 2003; DOI: 10.1137/1.9780898718003.
- (43) Press, W. H. et al. *Numerical Recipes: The Art of Scientific Computing*, 3rd ed.; Cambridge University Press: Cambridge, England, 2007.
- (44) Poirier, B. Using wavelets to extend quantum dynamics calculations to ten or more degrees of freedom. *J. Theor. Comput. Chem.* **2003**, *2*, 65.
- (45) Poirier, B.; Salam, A. Quantum dynamics calculations using symmetrized, orthogonal Weyl-Heisenberg wavelets with a phase space truncation scheme. II. Construction and optimization. *J. Chem. Phys.* **2004**, *121*, 1690–1703.
- (46) Poirier, B.; Salam, A. Quantum dynamics calculations using symmetrized, orthogonal Weyl-Heisenberg wavelets with a phase space truncation scheme. III. Representations and calculations. *J. Chem. Phys.* **2004**, *121*, 1704–1724.
- (47) Lombardini, R.; Poirier, B. Improving the accuracy of Weyl-Heisenberg wavelet and symmetrized Gaussian representations using customized phase-space-region operators. *Phys. Rev. E* **2006**, *74*, 036705
- (48) Pandey, A.; Poirier, B. An algorithm to find (and plug) "holes" in multi-dimensional surfaces. *J. Chem. Phys.* **2020**, *152*, 214102.
- (49) Pandey, A.; Poirier, B. Plumbing Potentials for Molecules with Up To Tens of Atoms: How to Find Saddle Points and Fix Leaky Holes. *J. Phys. Chem. Lett.* **2020**, *11*, 6468–6474.
- (50) Light, J.; Carrington, T., Jr. Discrete-variable representations and their utilization. *Adv. in Chem. Phys.* **2007**, *114*, 263–310.
- (51) Sarka, J.; Petty, C.; Poirier, B. Exact bound rovibrational spectra of the neon tetramer. *J. Chem. Phys.* **2019**, *151*, 174304.
- (52) Chen, W.; Poirier, B. Quantum Dynamical Calculation of All Rovibrational States of HO_2 for Total Angular Momentum J = 0 to 10. J. Theor. Comput. Chem. **2010**, 9, 435.
- (53) Petty, C.; Chen, W.; Poirier, B. Quantum Dynamical Calculation of Bound Rovibrational States of HO_2 up to Largest Possible Total Angular Momentum, $J \le 130$. *J. Phys. Chem. A* **2013**, *117*, 7280–7297.

- (54) Petty, C.; Poirier, B. Comparison of J-shifting Models for Rovibrational Spectra as Applied to the HO₂ Molecule. *Chem. Phys. Lett.* **2014**, 605–606, 16–21.
- (55) Yang, B.; Chen, W.; Poirier, B. Rovibrational Bound States of Neon Trimer: Quantum dynamical calculation of all eigenstate energy levels and wavefunctions. *J. Chem. Phys.* **2011**, *135*, 094306.
- (56) Brandon, D.; Poirier, B. Accurate calculations of bound rovibrational states for argon trimer. J. Chem. Phys. 2014, 141, 034302.
- (57) Yang, B.; Poirier, B. Quantum dynamical calculation of rovibrational bound states of Ne₂Ar. *J. Phys. B: At., Mol. Opt. Phys.* **2012**, 45, 135102.
- (58) Yang, B.; Poirier, B. Rovibrational Bound States of the Ar₂Ne Complex. J. Theor. Comput. Chem. **2013**, 12, 1250107.
- (59) Kumar, P.; Jiang, B.; Guo, H.; Klos, J.; Alexander, M. H.; Poirier, B. Photoabsorption Assignments for the $\tilde{C}^1B_2 \leftarrow \tilde{X}^1A_1$ Vibronic Transitions of SO₂, Using New ab initio Potential Energy and Transition Dipole Surfaces. *J. Phys. Chem. A* **2017**, *121*, 1012–1021.
- (60) Petty, C.; Spada, R. F.; Machado, F. B.; Poirier, B. Accurate rovibrational energies of ozone isotopologues up to J = 10 utilizing artificial neural networks. *J. Chem. Phys.* **2018**, *149*, 024307.
- (61) Sarka, J.; Poirier, B. Comment on "Calculated Vibrational States of Ozone up to Dissociation" [J. Chem. Phys. 144, 074302 (2016)]. J. Chem. Phys. 2020, 152, 177101.
- (62) Sarka, J.; Das, D.; Poirier, B. Calculation of rovibrational eigenstates of H₃⁺ using ScalIT. *AIP Adv.* **2021**, *11*, 045033.
- (63) Zhang, Z.; Li, B.; Shen, Z.; Ren, Y.; Bian, W. Efficient quantum calculation of the vibrational states of acetylene. *Chem. Phys.* **2012**, *400*, 1–7
- (64) Poirier, B.; Light, J. C. Phase Space Optimization of Quantum Representations: Direct-product basis sets. *J. Chem. Phys.* **1999**, *111*, 4869.
- (65) Poirier, B.; Light, J. C. Phase space optimization of quantum representations: Three-body systems and the bound states of HCO. *J. Chem. Phys.* **2001**, *114*, 6562.
- (66) Poirier, B. Phase Space Optimization of Quantum Representations: Non-Cartesian Coordinate Spaces. Found. Phys. **2001**, *31*, 1581.
- (67) Bian, W.; Poirier, B. Accurate and Highly Efficient Calculation of the O(¹D)HCl Vibrational Bound States, Using a Combination of Methods. *I. Theor. Comput. Chem.* **2003**, *2*, 583.
- (68) Huang, S.-W.; Carrington, T. A new iterative method for calculating energy levels and wave functions. *J. Chem. Phys.* **2000**, *112*, 8765–8771.
- (69) Poirier, B.; Carrington, T. Accelerating the Calculation of Energy Levels and Wave-functions, Using an Efficient Preconditioner with the Inexact Spectral Transform Method. *J. Chem. Phys.* **2001**, *114*, 9254–9264.
- (70) Poirier, B.; Carrington, T. A Preconditioned Inexact Spectral Transform Method for Calculating Resonance Energies and Widths, as applied to HCO. *J. Chem. Phys.* **2002**, *116*, 1215–1227.
- (71) Poirier, B.; Miller, W. H. Optimized Preconditioners for Green's Function Evaluation in Quantum Reactive Scattering Calculations. *Chem. Phys. Lett.* **1997**, 265, 77–83.
- (72) Poirier, B. Optimal Separable Bases and Series Expansions. *Phys. Rev. A: At., Mol., Opt. Phys.* **1997**, *56*, 120–130.
- (73) Poirier, B. Quantum Reactive Scattering for Three-Body Systems via Optimized Preconditioning, as Applied to the O+HCl Reaction. *J. Chem. Phys.* **1998**, *108*, 5216–5224.
- (74) Poirier, B. Efficient Preconditioning Scheme for Block Partitioned Matrices with Structured Sparsity. *Numer. Linear Algebra Appl.* **2000**, *7*, 715–726.
- (75) Ren, Y.; Li, B.; Bian, W. Full-dimensional quantum dynamics study of vinylidene acetylene isomerization: a scheme using the normal mode Hamiltonian. *Phys. Chem. Chem. Phys.* **2011**, *13*, 2052–2061.
- (76) Lill, J. V.; Parker, G. A.; Light, J. C. Discrete variable representations and sudden models in quantum scattering theory. *Chem. Phys. Lett.* **1982**, *89*, 483.

- (77) Light, J. C.; Hamilton, I. P.; Lill, J. V. Generalized discrete variable approximation in quantum mechanics. *J. Chem. Phys.* **1985**, *82*, 1400
- (78) Lill, J. V.; Parker, G. A.; Light, J. C. The discrete variable-finite basis approach to quantum scattering. *J. Chem. Phys.* **1986**, 85, 900.
- (79) Littlejohn, R. G.; Cargo, M.; Carrington, T., Jr.; Mitchell, K. A.; Poirier, B. A General Framework for Discrete Variable Representation Basis Sets. *J. Chem. Phys.* **2002**, *116*, 8691–8703.
- (80) Harris, D. O.; Engerholm, G. G.; Gwinn, W. D. Calculation of Matrix Elements for One-Dimensional Quantum-Mechanical Problems and the Application to Anharmonic Oscillators. *J. Chem. Phys.* **1965**, 43, 1515–1517.
- (81) Dickinson, A. S.; Certain, P. R. Calculation of Matrix Elements for One-Dimensional Quantum-Mechanical Problems. *J. Chem. Phys.* **1968**, *49*, 4209–4211.
- (82) Duncan, J. L.; McKean, D. C.; Tullini, F.; Nivellini, G. D.; Peña, J. Methyl cianide: Spectroscopic studies of isotopically substituted species, and the harmonic potential function. *J. Mol. Spectrosc.* **1978**, 69, 123.
- (83) Nakagawa, I.; Shimanouchi, T. Rotation-vibration spectra and rotational, Coriolis coupling, centrifugal distortion and potential constants of methyl cyanide. *Spectrochim. Acta* **1962**, *18*, 513.
- (84) Henry, L.; Amat, G. The cubic anharmonic potential function of polyatomic molecules. *J. Mol. Spectrosc.* **1961**, *5*, 319.
- (85) Henry, L.; Amat, G. The quartic anharmonic potential function of polyatomic molecules. *J. Mol. Spectrosc.* **1965**, *15*, 168.
- (86) Hoy, A. R.; Mills, I. M.; Strey, G. Anharmonic force constant calculations. *Mol. Phys.* **1972**, *24*, 1265.
- (87) Pouchan, C.; Zaki, K. Ab initio configuration interaction determination of the overtone vibrations of methyleneimine in the region 2800–3200 cm⁻¹. *J. Chem. Phys.* **1997**, *107*, 342.
- (88) Ischtwan, J.; Collins, M. A. Molecular Potential Energy Surfaces by Interpolation. *J. Chem. Phys.* **1994**, *100*, 8080–8088.
- (89) Metz, M. P.; Szalewicz, K.; Piszczatowski, K. Automatic Generation of Intermolecular Potential Energy Surfaces. *J. Chem. Theory Comput.* **2016**, *12*, 5895–5919.
- (90) Quintas-Sánchez, E.; Dawes, R. AUTOSURF: A freely available program to construct potential energy surfaces. *J. Chem. Inf. Model.* **2019**, 59, 262–271.
- (91) Györi, T.; Czakó, G. Automating the Development of High-Dimensional Reactive Potential Energy Surfaces with the ROBOSUR-FER Program System. *J. Chem. Theory Comput.* **2020**, *16*, 51–66.